

Compressibility and rarefaction effects on entropy and entropy generation in micro/nano Couette flow using DSMC

This article has been downloaded from IOPscience. Please scroll down to see the full text article.

2012 J. Phys.: Conf. Ser. 362 012008

(<http://iopscience.iop.org/1742-6596/362/1/012008>)

View [the table of contents for this issue](#), or go to the [journal homepage](#) for more

Download details:

IP Address: 95.211.165.66

The article was downloaded on 14/08/2012 at 07:58

Please note that [terms and conditions apply](#).

Compressibility and rarefaction effects on entropy and entropy generation in micro/nano Couette flow using DSMC

Omid Ejtehadi, Javad Abolfazli Esfahani, Ehsan Roohi¹

Department of Mechanical Engineering, Faculty of Engineering, Ferdowsi university of Mashhad, Mashhad, Iran, P.O. Box: 91775-1111

Abstract. In the present work, compressible flow of argon gas in the famous problem of Couette flow in micro/nano-scale is considered and numerically analyzed using the direct simulation Monte Carlo (DSMC) method. The effects of compressibility and rarefaction on entropy and entropy generation in terms of viscous dissipation and thermal diffusion are studied in a wide range of Mach and Knudsen numbers and the observed physics are discussed. In this regard, we computed entropy by using its kinetic theory formulation in a microscopic way while the entropy generation distribution is achieved by applying a semi-microscopic approach and thoroughly free from equilibrium assumptions. The results of our simulations demonstrated that the entropy profiles are in accordance with the temperature profiles. It is also illustrated that the increase of Mach number will result in non-uniform entropy profiles with increase in the vicinity of the central regions of the channel. Moreover, generation of entropy in all regions of the domain stages clear growth. By contrast, increasing the Knudsen number has inverse effects such as: uniform entropy profiles and a falling off in entropy generation amount throughout the channel.

1. Introduction

In recent years, prediction of rarefied gas flows and heat transfer behaviour attracted attention due to the wide application of micro/nano electromechanical system (MEMS/NEMS) devices such as micro/nano- valve, micro/nano- turbine, micro/nano- pump and micro/nano- nozzle. Moreover, many experimental, numerical and theoretical studies have been conducted in the field [1-6]. Rarefied shear-driven flows such as Couette are encountered in micro-motor, comb mechanism, and micro-bearing. To measure the degree of rarefaction the Knudsen number (Kn) is defined as the ratio of mean free path of gas molecules to the characteristic length of the geometry ($Kn=\lambda/L$). When the Knudsen number is sufficiently large, the gas rarefaction is the main parameter to evaluate these systems.

In this study we consider the entropy and entropy generation of the well known problem of planar Couette flow, i.e., a gas confined between two infinite parallel plates which are at the same temperature but moving relative to each other. The advantage of studying Couette flow is that despite it is a relatively simple problem it includes many features found in more complex rarefied gas dynamics problems. The micro/nano-Couette flow has been widely applied in existing literature for different purposes. Some of the sample works can be found in [7-14]. Meanwhile, entropy and entropy generation concepts are widely used in the literature for different important purposes such as: evaluating a system's irreversibility, optimizing a thermodynamic system or as a means of examining

¹ Corresponding Author: Ehsan Roohi, Assistant Professor, Tel.: +98-511-8805136, Fax: +98-511-8763304, Email: e.roohi@ferdowsi.um.ac.ir

continuum breakdown in rarefied fluids. For example: Reitebuch and Weiss [15] employed a new min-max principle for the entropy production to determine more boundary conditions. They used 26 field equations derived by the moment method to describe the stationary plane Couette flow for dense and rarefied gases. Their new boundary conditions results in a heat flux in the direction of the flow which agrees with molecular dynamics results. Ansumali and Karlin [16] implemented the lattice Boltzmann method based on the H theorem (entropic lattice Boltzmann method) for a one-dimensional benchmark shock tube problem. Results of their simulation demonstrate significant improvement of stability, as compared to realizations without explicit entropic estimations. Schrock et al. [17-19] expanded upon the concept of entropy generation as a means of examining the breakdown of the continuum fluid equations in regions of non-equilibrium. They compared the DSMC result with those obtained by numerically integrating the NS equations in normal shock waves. They have shown that significant non-equilibrium may exist upstream of any indication of such phenomena in the NS data in the case of the normal shock. They also stated that any breakdown parameter based on the continuum data will fail to capture the initial onset of the shock front. Carr [20] introduced a new method for calculating entropy generation using the DSMC method to investigate the limits of the continuum constitutive relations. He compared continuum results with the DSMC solution for the hypersonic flow over two axisymmetric geometries and showed that the kinetic method predicts a larger shock region than the continuum method. Erbay et al. [21] investigated the effects of aspect ratio, Reynolds number (Re), Prandtl number (Pr), Brinkman number (Br), and the motion of the lower plate on the entropy generation during the simultaneously developing flow in a parallel-plates channel. They showed that entropy generation has its highest value at channel with the smallest aspect ratio at counter motion of the lower plate while the highest Re , Pr and Br/Ω values considered in the problem. Ozlap [22] numerically investigated entropy generation for laminar fully developed, forced convection in a micro-pipe. The simulations were concentrated on the impact of wall roughness based viscous dissipation on the heat transfer behaviour and the resulting overall and radial entropy generation. In another work, Ozlap [23] investigated entropy generation for wide ranges of pipe diameter ($d = 0.5 - 1mm$), wall heat flux ($q'' = 1000 - 2000 \text{ w/m}^2$) and Reynolds number ($Re = 1 - 2000$). He concludes that the cross-sectional total entropy generation is computed to be most influenced by pipe diameter at high wall heat flux and low Reynolds numbers. Ozlap [24] also studied the integrated effects of surface roughness, heat flux, and Reynolds number on the first and second law characteristics of laminar-transitional flow in a micropipe and showed that the frictional entropy is minor and the major portion of the total entropy generation is thermal based. Chigullapalli et al. [25] formulated and applied a discrete version of the Boltzmann's H-theorem for analysis of non-equilibrium onset and accuracy of the numerical modelling of rarefied gas flows. They illustrated the use of entropy considerations in rarefied flow simulations for the normal shock, the Riemann and the two-dimensional shock tube problems. They stated that the entropy generation rate based on the kinetic theory is shown to be a powerful indicator of the onset of non-equilibrium, accuracy of numerical solution as well as the compatibility of boundary conditions for both steady and unsteady problems. Leite and Santos [26] investigated effect of the step back-face height on the thermal non-equilibrium in backward-facing steps in a rarefied hypersonic flow using DSMC. They showed that entropy generation regions are related to the thermal non-equilibrium regions in the flow field. Parlak et al. [27] studied steady-laminar flow of water in adiabatic microtubes experimentally and analytically. Through employing the second law analysis, they showed that the flow characteristics in the smooth microtubes distinguish substantially from the conventional theory for flow in larger tubes with respect to viscous heating/dissipation, temperature rise of flow, total entropy generation rate and lost work.

It is observed that there is a great deal of papers dealing with the entropy generation analysis in high Knudsen number simulations; however, the entropy and entropy generation analysis of the micro/nano-Couette flow is not implemented by DSMC method yet. The present work is following the previous works by authors regarding DSMC simulations [28-30] and second law analysis [31-33]. Here, the compressible micro/nano-Couette flow is studied with a special focus on entropy and

entropy generation profiles. Compressibility and rarefaction effects in a wide range of Mach and Knudsen numbers are investigated. The results are then discussed and justified to obtain a better knowledge of the system behaviour regarding the second law analysis.

2. Numerical analysis

2.1. Problem statement

Planar Couette flow involves a gas trapped between two infinite plate at $y = \pm h / 2$ moving relative to each other in opposite directions with a constant velocity $\pm U_w$ and maintained at the same constant temperature, T_w . The flow is driven by the shear stress of the moving plates and depends on the y coordinate only. Therefore the flow is considered steady, one dimensional and compressible. The flow velocity generated by shear is assumed to have only an x component varying only in the y direction. Temperature profiles are parabolic and are generated by the viscous dissipation. The amount of heat flux in y direction is zero in the center of the channel and increases towards the plates. The shear stress in the domain is constant. Also the external forces are assumed to be absent. A schematic of the problem is depicted in Fig. 1.

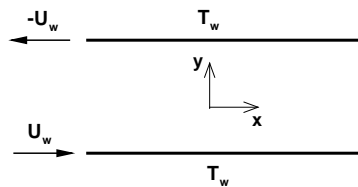


Figure 1. Schematic of the problem

2.2. DSMC method

The Boltzmann equation describes the gas flow behaviour in all the regimes. The DSMC method is proved to be the most accurate numerical tool to solve the Boltzmann equation based on direct statistical simulation of the molecular processes described by the kinetic theory [34]. In fact, DSMC simulates particle behaviour in a manner consistent with what is described by the Boltzmann equation. The algorithm includes four primary steps: moving the particles, indexing them, collision simulation, and sampling the flow-field. The primary principle of DSMC is to decouple the motion and collision of particles during one time step. The implementation of DSMC needs breaking down the computational domain into a collection of grid cells. The cells are divided into subcells in each direction. The subcells are then utilized to facilitate the selection of collision pairs. After fulfilling all molecular movements, the collision between molecules are simulated in each cell separately in a statistical manner. Accurate DSMC solution requires some constraints on the cell size, time step and number of particles. The random selection of the particles from a cell for binary collisions requires that the cell size to be a small fraction of the gas mean free path. The decoupling between the particles movement and collisions is correct if the time step is a small fraction of the mean collision time. Number of particles per cell should be high enough, around 20, to avoid repeated binary collisions between the same particles. The following procedure is used to solve a stationary problem with DSMC. In the entire computational domain, an arbitrary initial state of gas particles is specified and the desired boundary conditions are imposed at time zero. Particles movement and binary collisions are performed separately. After achieving steady flow condition, sampling of molecular properties within each cell is fulfilled during sufficient time period to avoid statistical scattering. All thermodynamic parameters such as temperature, velocity, density and pressure are then determined from this time-averaged data. More details on DSMC algorithm are given in Refs. [34-35]. In the current study, a modified version of Bird's DSMC2D program is applied and periodic boundary conditions are imposed for left and right boundaries such that one-dimensional Couette flow is

simulated. Variable hard sphere (VHS) collision model is used and the collision pair is chosen based on the no time counter (NTC) method. We use diffuse reflection model with the full thermal accommodation coefficient for the walls and set the time step and cell dimensions equal to 10^{-13} (s) and 10^{-8} (m), respectively. These values are set in such a way that they do not exceed one third of collision time and mean free path, respectively.

3. Results and discussion

3.1. Entropy

The second law of thermodynamics states that entropy of an isolated system always increases or remains constant. The second thermodynamic law appears to establish the direction that the heat flux will occur, say, the direction will be that one where $\Delta s > 0$. Because such a process acts to reduce the initial state of the order of the system, entropy is in conjunction with disorder or randomness especially in microscopic interpretation of entropy in statistical mechanics. We can also deal with entropy as of thermal energy dispersal. The relation of entropy as a measure of disorder is Boltzmann relation for the entropy [36]:

$$S = k_B \ln \Omega \quad (1)$$

where k_B is the Boltzmann constant, equal to 1.38065×10^{-23} (J/K) and Ω the number of possible microstates in the system called degeneracy or statistical multiplicity of the gas, respectively. In fact, entropy is a logarithmic measure of the density of microstate which characterizes all molecular details about the system such as molecular position and velocity. It can be stated as a summation over all microstates that a system can be in:

$$S = -k_B \sum_i f_i \ln(f_i) \quad (2)$$

In the above equation, f_i is the probability that the system is in the i^{th} microstate.

Here, because of the availability of the data in the DSMC solver, we use a velocity distribution function in order to calculate entropy. It is assumed that the velocity distribution could be separated into a product of the component distributions, that is:

$$f(\mathbf{c}) = f_x(c_x) f_y(c_y) f_z(c_z) \quad (3)$$

The velocity spectrum is divided into bins and the number of molecules associated with each bin is counted to form the above distribution function. Entropy is then calculated based on the above procedure and Eq. (2). For detailed information regarding implementing the method see Ref. [17, 18]

3.1.1. Compressibility effects

The wall Mach number, M_w , is defined as the ratio of U_w to the parameter $\sqrt{\gamma k_B T_w / m}$ and is specified by varying driving velocity of both plates U_w . Here, γ and m are specific heat ratio of gas and molecular mass, respectively.

Figure 2 illustrates the variation of temperature in the domain with wall Mach variation. The temperature profiles show that as M_w increases, the temperature difference between the plates and center of channel becomes larger due to higher viscous dissipation. Thus, compressibility effects become significant. The growth of temperature jump at the walls by increasing the Mach number is quite obvious in Fig. 2. The magnitude of the temperature jump at $M_w=1.2$ is almost 20% of the wall temperature.

Compressibility effects on entropy profiles are illustrated in Fig. 3. Comparison of Figs. 2 and 3 reveals that these two quantities follow a same trend, i.e., a parabolic profile with the maximum value at the center of the channel. This is because the heat is a disordered form of energy and flows with the entropy. Consequently, entropy or molecular chaos increases in the regions of higher temperature. This extremum swells as Mach increases. This is due to the existence of higher molecular chaos as a result of the greater number of microstates in the middle of the channel. In fact, existence of less number of molecules leads to smaller amount of intermolecular collisions. Hence, the molecules are not able to balance their energy level as it is in near-wall regions. It is also apparent that the plates'

movement in the x direction organizes adjacent molecules to the plates in such a way that the implications are less entropy (disorder) in the vicinity of the walls. As this velocity increases, the order of molecules near the plates is more obvious resulting in less entropy compared to the disorder at the channel center.

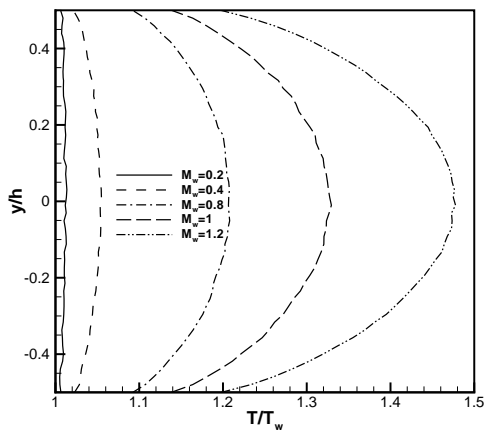


Figure 2. Compressibility effects on non-dimensional temperature profiles ($Kn=0.1$)

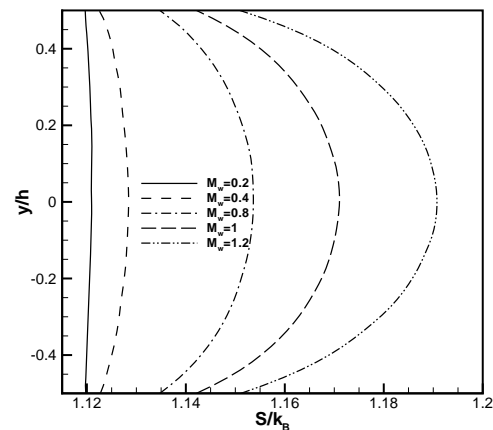


Figure 3. Compressibility effects on non-dimensional entropy profiles ($Kn=0.1$)

3.1.2. Rarefaction effects

Rarefaction effects gain importance with the reduction in the geometry size, since the sizes of the geometries become comparable to the mean free path of the gas molecules. These effects are specified through the Knudsen number. Now, the plates' velocity is kept constant ($U_w=250$ m/s) and the corresponding wall Mach numbers is 0.81.

Due to the similarities between entropy and temperature profiles discussed in the previous section, first and foremost, temperature variations with Knudsen number are investigated. Figure 5 illustrates the temperature profiles at different Knudsen numbers. As the Knudsen number increases, temperature in the domain and also temperature jump at the plates becomes more significant, but the curvature of temperature profiles reduces. In a constant wall Mach number flow, the amount of wall kinetic energy is constant. As the flow becomes more rarefied, this constant kinetic energy will be saved in smaller number of the molecules and shows itself in term of temperature rise. However, in a dense gas this amount of constant energy is distributed in larger number of molecules and the temperature rise is smaller than what is observed in rarefied gases. Also for small Knudsen numbers and close to the continuum regime, only near surface molecules collide with the walls and in the middle of channel only the intermolecular collisions happen. For larger Knudsen numbers, as the gas becomes more rarefied, molecules in the middle of channel have the same chance for molecular-surface collision and transferring heat from/to the walls. Consequently, the maximum curvature in Fig. 4 is observed in the $Kn=0.01$ and by increase of the Knudsen number the temperature in the domain becomes uniform.

Figure 5 shows rarefaction effects on entropy profiles. It can be seen from the graph that the curvature in the entropy diagrams subsides as the Knudsen number increases. This is because of occupation of the domain by the Knudsen layer, a kinetic boundary layer on the order of one mean free path, for more rarefied flows. We can also see that the trend is quite similar to the observed trends in temperature profiles. Therefore, as a general conclusion we could state that the more rarefied flow, more uniform entropy profiles are observed. The justification for this conclusion is the more uniform distribution of the molecules in the domain for rarefied flows rather than dense gases. Therefore, the distribution of energy in molecules is more balanced.

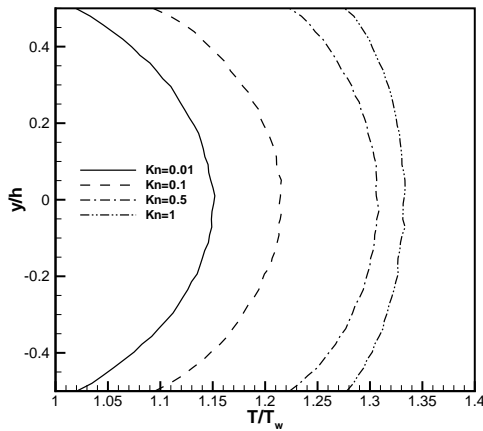


Figure 4. Rarefaction effects on non-dimensional temperature profiles ($M_w=0.81$)

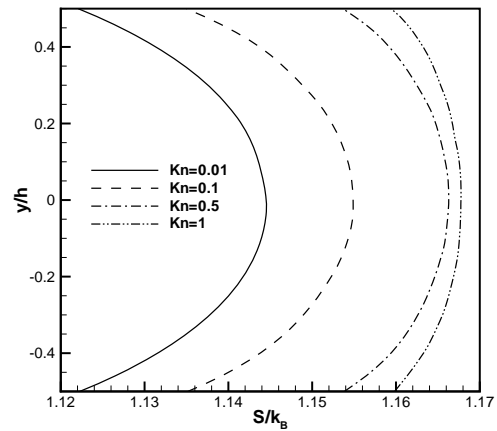


Figure 5. Rarefaction effects on non-dimensional entropy profiles ($M_w=0.81$)

3.2. Entropy generation

Studies of Schrock et al. [17-19] state that because entropy generation represents non-equilibrium it can be employed as a similar parameter to the Knudsen number. Therefore it will predict the continuum breakdown onset. They also showed that breakdown parameters based upon continuum data may fail to capture the initial non-equilibrium effects. Their investigation showed that it is necessary to develop a formulation for entropy generation based on kinetic theory and without inherent assumptions of equilibrium built in to be able to measure the small perturbations from non-equilibrium observed in the NS equations. Therefore, they proposed expressions for entropy and entropy generation in terms of the distribution functions of velocity, rotational energy, and vibrational energy. The DSMC method was applied in their work to generate these distribution functions. A theoretically accurate but computationally expensive and difficult method due to the necessity of sorting particles to create the distribution functions was employed in their work. For this reason, a different approach for calculating entropy generation proposed by Carr [20] has been used here, eliminating the need to sort particles into distribution functions. In this method a constitutive relation valid in equilibrium is applied. However, by replacing the parameters which are calculated by the DSMC solution, the final relation for entropy generation will be free from assumptions of equilibrium.

$$\dot{S}_{gen} = \frac{\tau_{ij}}{T} \frac{\partial u_i}{\partial x_j} - \frac{q_i}{T^2} \frac{\partial T}{\partial x_i} \quad (4)$$

In the above equation τ_{ij} and q_i are the shear stress and heat flux, respectively. Because of the equilibrium assumptions made in the constitutive relations for the shear stress and heat flux in the NS equation, the corresponding relations for these quantities in the kinetic theory will be used:

$$\boldsymbol{\tau} = \tau_{ij} = -(\rho \overline{c'_i c'_j} - \delta_{ij} \mathbf{p}) \quad (5)$$

where c'_i and c'_j are the components of \mathbf{c}' , the velocity of molecule relative to stream velocity, i.e., thermal velocity and \mathbf{p} is the scalar pressure defined as:

$$\mathbf{p} = p_{ij} = \rho \overline{c'_i c'_j} \quad (6)$$

The heat flux vector is defined as:

$$\mathbf{q} = \frac{1}{2} \rho \overline{c'^2 \mathbf{c}'} + n \overline{\varepsilon_{int} \mathbf{c}'} \quad (7)$$

where, ε_{int} is the internal energy of a single molecule.

Finally, the entropy generation derivation for the one-dimensional Couette flow according to [20] becomes:

$$\begin{aligned}\dot{S}_{gen} &= \frac{\tau_{ij}}{T} \frac{\partial u_i}{\partial x_j} - \frac{q_i}{T^2} \frac{\partial T}{\partial x_i} \\ &= \frac{\tau_{xx}}{T} \frac{\partial u}{\partial x} - \frac{q_x}{T^2} \frac{\partial T}{\partial x} + \frac{\tau_{xy}}{T} \frac{\partial u}{\partial y} - \frac{q_x}{T^2} \frac{\partial T}{\partial x} + \frac{\tau_{yx}}{T} \frac{\partial v}{\partial x} - \frac{q_y}{T^2} \frac{\partial T}{\partial y} + \frac{\tau_{yy}}{T} \frac{\partial v}{\partial y} - \frac{q_y}{T^2} \frac{\partial T}{\partial y}\end{aligned}\quad (8)$$

Where, both i and j are representative of x and y , sequentially. Since there is no velocity and temperature gradients in x direction the final expression for entropy generation yields:

$$\dot{S}_{gen} = \frac{\tau_{xy}}{T} \frac{\partial u}{\partial y} - 2 \frac{q_y}{T^2} \frac{\partial T}{\partial y}\quad (9)$$

In the above equation the first term is called the generation of entropy due to viscous dissipation shown by S_μ and the second due to thermal diffusion represented by S_D .

3.2.1. Compressibility effects

Owing to the fact that entropy generation can be treated as a means of quantifying non-equilibrium, first density variation are investigated to look for similarities in these quantities. Figure 6 illustrates the normalized density profiles for different Mach numbers. It is clear from the graph that as the Mach increases the density profiles deviate from the uniform distribution. It is also observed that the amount of density is in its minimum at the center of the channel for all Mach numbers.

Figure 7 shows the compressibility effects on the entropy generation profiles. The figure shows that more entropy is generated in near wall regions where the Knudsen layer is formed. Here the flow is less rarefied than the center of the channel. It is also observed that for higher wall Mach numbers production of entropy in whole regions of the domain increases which is the result of viscous heating, caused by the more kinetic energy absorbed from the wall moving in higher speeds.

In Figs. 8 and 9 each term of Eq. (9) is plotted separately. The comparison of these two figures shows that the generated entropy in the domain is mainly influenced by the viscous dissipation term, S_μ rather than thermal diffusion term, S_D . However, the latter is the main cause for non-uniform entropy generation profiles due to large temperature gradients in the vicinity of the walls.

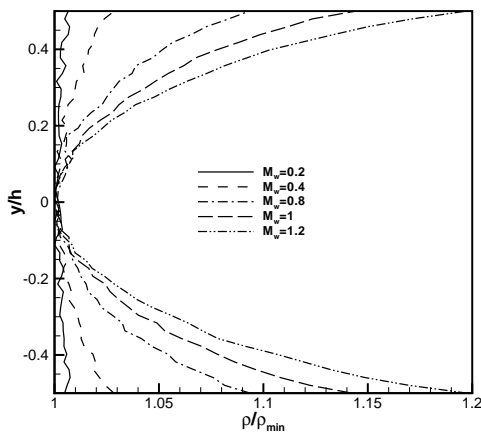


Figure 6. Compressibility effects on non-dimensional density profiles (Kn=0.1)

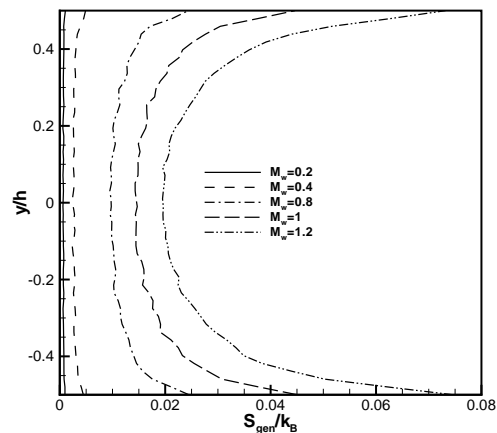


Figure 7. Compressibility effects on non-dimensional entropy generation profiles (Kn=0.1)

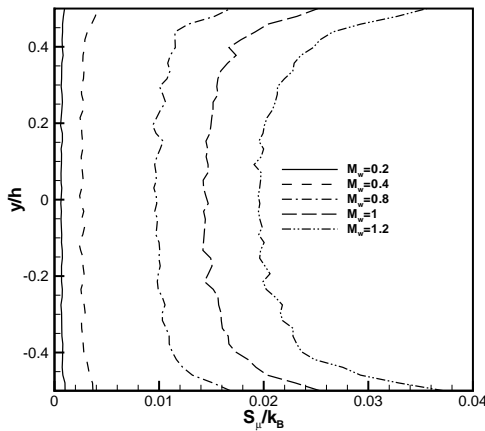


Figure 8. Compressibility effects on non-dimensional viscous dissipation term of the entropy generation profiles ($Kn=0.1$)

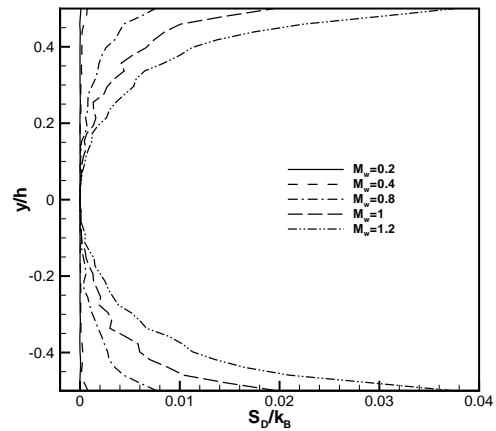


Figure 9. Compressibility effects on non-dimensional thermal diffusion term of the entropy generation profiles ($Kn=0.1$)

3.2.2. Rarefaction effects

Variation of non-dimensional density profiles for different Knudsen numbers is plotted in Fig. 10. It is obvious that increase in the Knudsen number leads to decrease in density. Also the non-dimensional density profiles tend to uniform profiles in more rarefied simulations as a result of development of the Knudsen layer in the entire domain.

In Fig. 11 the profiles of entropy generation for different Knudsen numbers confirms the expected trends in density profiles. The figure reveals that in a more rarefied flow less entropy is generated. It is also observed that for smaller Knudsen numbers ($Kn < 0.5$) the distribution of entropy generation is non-uniform in the domain. However, as the Knudsen number increases higher percentage of the channel area is occupied by the Knudsen layer resulting in uniform profiles of entropy generation. Figures 12 and 13 show how the generation of entropy is distributed in the viscous dissipation and thermal diffusion terms. It can be concluded that this parameter is mainly a result of the viscous dissipation term than thermal diffusion. This effect is greater in dense gases rather than in rarefied gases. Also it is apparent from Fig. 13 that the thermal diffusion is the cause of non-uniform profiles of entropy generation.

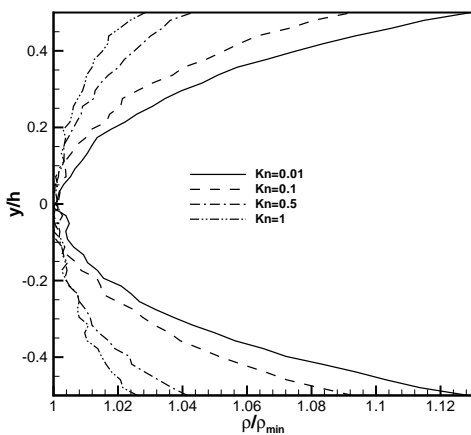


Figure 10. Rarefaction effects on non-dimensional density profiles ($M_w=0.81$)

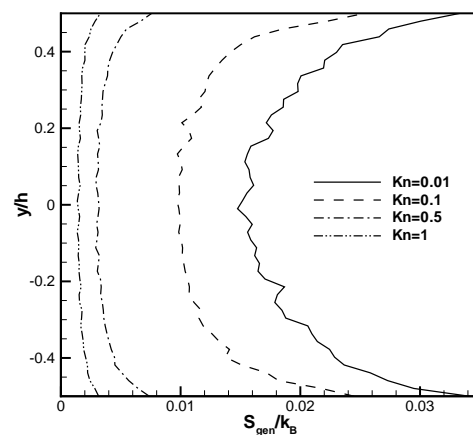


Figure 11. Rarefaction effects on non-dimensional entropy generation profiles ($M_w=0.81$)

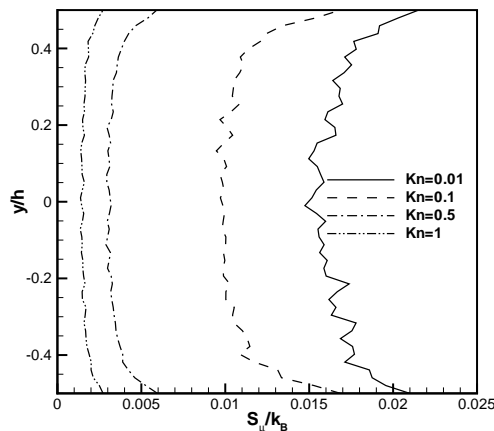


Figure 12. Rarefaction effects on non-dimensional viscous dissipation term of the entropy generation profiles ($M_w=0.81$)

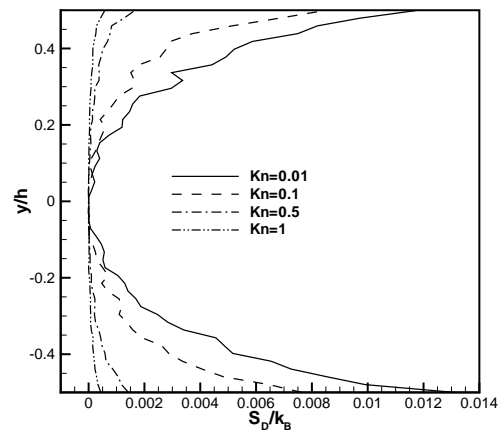


Figure 13. Rarefaction effects on non-dimensional thermal diffusion term of the entropy generation profiles ($M_w=0.81$)

4. Concluding remarks

Simulating the rarefied flow of argon gas in the famous problem of Couette flow, compressibility and rarefaction effects on entropy and entropy generation profiles are investigated using the DSMC method. The main concluding remarks of the present work include:

- ❖ Investigation of compressibility effects shows that increase of wall Mach number results in non-uniform entropy profiles with a peak in the center of the channel and more generation of entropy in whole regions of the channel because of the viscous heating. The results also reveal that entropy and temperature profiles are following an identical trend.
- ❖ Investigation of rarefaction effects shows that increase of Knudsen number results in more uniform entropy profiles.
- ❖ Considering the entropy generation profiles along with density profiles, it can be perceived that this quantity can be properly applied in quantifying non-equilibrium phenomena not only in hypersonic flows as stated in the existing literature, but also in low Reynolds micro/nano flows.
- ❖ It is shown that in the micro-Couette flow the generation of entropy is mainly due to viscous dissipation term observed in the final derived equation. However, the issue that causes more non-uniform profiles is the thermal diffusion term.

Acknowledgement

The authors of the paper would like to acknowledge the financial supports of the Ferdowsi University of Mashhad under grant number 20522.

References

- [1] Ho C-M and Tai Y-C 1998 Micro-electro-mechanical-systems (MEMS) and fluid flows *Annual Review of Fluid Mechanics* **30** 579-612
- [2] Reese J M, Gallis M A and Lockerby D A 2003 New directions in fluid dynamics: Non-equilibrium aerodynamic and microsystem flows *Philosophical Transactions of the Royal Society of London. Series A: Mathematical, Physical and Engineering Sciences* **361** 2967-2988
- [3] Darhuber A A and Troian S M 2005 Principles of microfluidic actuation by modulation of surface stresses *Annual Review of Fluid Mechanics* **37** 425-455

- [4] Karniadakis G, Beskok A and Aluru N 2005 *Micro flows and nano flows: Fundamentals and simulation* (New York, Springer-Verlag)
- [5] Tabeling P 2005 *Introduction to microfluidics* (New York, Oxford University Press)
- [6] Liou W W and Fang Y 2006 *Microfluid mechanics: Principles and modelling* McGraw-Hill)
- [7] Willis D 1962 Comparison of kinetic theory analyses of linearized Couette flow *Phys. Fluids* **5** 127
- [8] Beskok A, Karniadakis G E and Trimmer W 1996 Rarefaction and compressibility effects in gas microflows *Journal of Fluids Engineering* **118** 448-456
- [9] Xue H, Fan Q and Shu C 2000 Prediction of micro-channel flows using direct simulation Monte Carlo *Probabilistic Engineering Mechanics* **15** 213-219
- [10] Xue H, Ji H M and Shu C 2001 Analysis of micro-Couette flow using the Burnett equations *International Journal of Heat and Mass Transfer* **44** 4139-4146
- [11] Roy S and Chakraborty S 2007 Near-wall effects in micro scale Couette flow and heat transfer in the maxwell-slip regimes *Microfluidics and Nanofluidics* **3** 437-449
- [12] Frezzotti A and Gibelli L 2008 A kinetic model for fluid-wall interaction *Proceedings of the Institution of Mechanical Engineers, Part C: Journal of Mechanical Engineering Science* **222** 787-795
- [13] Gu X J and Emerson D R 2009 A high-order moment approach for capturing non-equilibrium phenomena in the transition regime *Journal of Fluid Mechanics* **636** 177-216
- [14] Kumar, Rakesh, Titov, V. E, Levin and A. D 2010 Reconsideration of planar Couette flows using the statistical bhatnagar-gross-krook approach *Anglais* **24** 9
- [15] Reitebuch D and Weiss W 1999 Application of high moment theory to the plane Couette flow *Continuum Mechanics and Thermodynamics* **11** 217-225
- [16] Ansumali S and Karlin I V 2000 Stabilization of the lattice Boltzmann method by the h theorem: A numerical test *Physical Review E* **62** 7999
- [17] Schrock, C.R. 2005 Entropy Generation as a Means of Examining Continuum Breakdown, Air Force Ins of Tech Wright-Patterson AFB OH School of Engineering and Management
- [18] Schrock C R and McMullan R J 2005 *Calculation of entropy generation rates via dsmc with application to continuum/equilibrium onset* 38th AIAA Thermophysics Conference Toronto, Ontario Canada
- [19] Schrock C R, McMullan R J and Camberos J A 2005 *Continuum onset parameter based on entropy gradients using Boltzmann's h-theorem* 43rd AIAA Aerospace Sciences Meeting and Exhibit Reno, Nevada
- [20] R.W. Carr, 2007 Quantifying non-equilibrium in hypersonic flows using entropy generation, Air Force Institute of Technology.
- [21] Erbay L, Yalçın M and Ercan M S 2007 Entropy generation in parallel plate microchannels *Heat and Mass Transfer* **43** 729-739
- [22] Ozalp A 2008 Roughness induced forced convective laminar-transitional micropipe flow: Energy and exergy analysis *Heat and Mass Transfer* **45** 31-46
- [23] Ozalp A A 2010 Combined effects of pipe diameter, Reynolds number and wall heat flux and on flow, heat transfer and second-law characteristics of laminar-transitional micro-pipe flows *Entropy* **12** 445-472
- [24] Ozalp A A 2009 1st and 2nd law characteristics in a micropipe: Integrated effects of surface roughness, heat flux and reynolds number *Heat Transfer Engineering* **30** 973-987
- [25] Chigullapalli S, Venkatraman A, Ivanov M S and Alexeenko A A 2010 Entropy considerations in numerical simulations of non-equilibrium rarefied flows *Journal of Computational Physics* **229** 2139-2158
- [26] Leite P H M and Santos W F N 2010 Thermal non-equilibrium effects on the flow field structure of hypersonic backward-facing step flow *Mecánica Computacional* **xxix** 4935-4953
- [27] Parlak N, Gür M, ArI V, Küçük H and Engin T 2010 Second law analysis of water flow through smooth microtubes under adiabatic conditions *Experimental Thermal and Fluid Science* **35** 60-67

- [28] Ejtehadi O, Roohi E and Esfahani J A 2011 *Dsmc simulation of micro/nano shear driven flows* The 10th Iranian Aerospace Society Conference Tehran Iran
- [29] Ejtehadi O, Roohi E and Esfahani J A 2012 Investigation of basic molecular gas structural effects on hydrodynamics and thermal behaviours of rarefied shear driven micro/nano flow using DSMC *International Communications in Heat and Mass Transfer* **39** 439-448
- [30] Roohi E and Darbandi M 2012 Recommendations on performance of parallel dsmc algorithm in solving subsonic nanoflows *Applied Mathematical Modelling* **36** 2314-2321
- [31] Esfahani J A and Jafarian M M 2005 Entropy generation analysis of a flat plate boundary layer with various solution methods *Scientia Iranica* **12** 233-240
- [32] Esfahani J A and Koochi-Fayegh S 2009 Entropy generation analysis in error estimation of an approximate solution: A constant surface temperature semi-infinite conductive problem *THERMAL SCIENCE* **13** 133-140
- [33] Esfahani J A and Shahabi P B 2010 Effect of non-uniform heating on entropy generation for the laminar developing pipe flow of a high prandtl number fluid *Energy Conversion and Management* **51** 2087-2097
- [34] Bird G A 1994 *Molecular gas dynamics and the direct simulation of gas flows* Clarendon Press, Oxford, United Kingdom)
- [35] Cercignani C 2000 *Rarefied gas dynamics. From basic concepts to actual calculations* Cambridge University Press)
- [36] Vincenti W G and Kruger C H 1967 *Introduction to physical gas dynamics* (New York, Wiley & Sons, Inc.)